Phase Feedforward Control For Single-Phase Boost-Type SMR

*Hung-Chi Chen (IEEE Member), **Chih-Kai Huang
*Department of Electrical and Control Engineering,
National Chiao Tung University, HsinChu, Taiwan.
**Industrial Technology Research Institute, HsinChu, Taiwan.

Abstract- **In this paper, the phase feedforward control (PFFC) for single-phase boost-type switching-mode-rectifier (SMR) is proposed. Compared to the fixed feedforward signal in the conventional feedforward control, the phase of the conventional feedforward signal now is controllable according to the load power which makes PFFC be able to yield more feedforward efforts for high load power. For implementing the high-sampling-frequency function of power factor correction (PFC) in low-cost DSP-based system or in digital integrated circuit, the economical proportional-type (P-type) feedback controller is used in the proposed PFFC instead of using the proportional-plus-integral-type (PI-type) feedback controller or other complicated controllers. In addition, we can use relatively small P-type parameter in the proposed PFFC which also increases the system stability. The analysis and design of proposed PFFC are described in detail. The simulation and experimental results also demonstrate the proposed PFFC. Target applications of the proposed PFFC are low-cost digital control for terrestrial 50-60Hz system whose performance is limited by the speed of the digital controller.**

I. INTRODUCTION

The AC/DC converter is an essential component for most power electronic systems to build up DC-link voltage source from the AC mains. The use of switching-mode-rectifier (SMR) with power factor correction (PFC) function is an effective mean to perform the AC/DC conversion with high input and output quality by shaping the input current waveform and regulating the output dc voltage. The boost-type SMRs are the most popular circuit topology among all the others to perform PFC functions for their continuous current in the front-end inductors [1-2].

Feedforward control is usually used to eliminate or reduce the effects of disturbances in a control system. It is also very useful in single-phase PFC applications with time-varying current references where input voltage feedforward has been successfully applied to eliminate the dependency of voltage loop gain on input root mean square voltage. In addition, in order to obtain better current tracking performance, many current controllers had been developed in the literatures, such as predictive control[3], mixed-mode control[4], robust current control[5] and feedback control [6,7]…. Most of them also include the feedforward loops in their current controller [3-7].

The basic idea of the conventional feedforward loop is to generate the "nominal duty ratio pattern" derived only from rectified input voltage in order to alleviate the task of the feedback controller. This nominal duty ratio pattern effectively produces a voltage across the switch whose average over a switching cycle is equal to the instantaneous rectified input voltage. A sinusoidal input current can then be produced by the feedback controller that changes the duty ratio around this nominal pattern according to current error. However, it is noted that this nominal duty ratio pattern is fixed regardless of load power. That is, the nominal duty ratio pattern generated in heavy load is the same as that in light load.

Therefore, in order to generate a flexible (i.e. load-dependent) feedforward signal to help the feedback controller, "full feedforward" in [7] and "load feedforward" in [8] had been developed. In the former, the feedforward signal is not only from the rectified input voltage but also from the inductor current command. Otherwise, in the latter, an additional load current must be sensed to generate the flexible feedforward signal. Both feedforward loops can provide more forward duty than the nominal one when the AC/DC system must yield larger power.

However, the full feedforward loop [7] is implemented in analog circuits but it is not suitable for the digital control system for the need of acceptable resolution in digital implementation. The need of sensing load current is the main disadvantage of the feedforward loop in [8]. For low-cost DSP-based system, implementation of the proportional-plus-integral-type (PI-type) controller in DSP-based environment needs more instructions than the proportional-type (P-type) controller. For digital integrated circuits, more circuits like "state machine" must be designed to implement PI-type controller than P-type controller. It implies that PI-type controllers are not suitable in low-cost digital control system.

The proposed PFFC consists of economical P-type feedback controller and the phase feedforward loop. Because the proposed phase feedforward loop can be simply implemented by the actions of looking-up table, the proposed PFFC can be referred to as one solution of high-switching-frequency PFC function implemented in the low-cost DSP-based system or digital integrated circuits. It is noted that the phase feedforward signal in PFFC is not to change the nominal pattern of duty ratio but to shift it. The larger the current magnitude is, the more the shifting phase of the nominal duty ratio pattern is.

978-1-4244-1874-9/08/$25.00 ©2008 IEEE

II. Conventional Feedforward Control

A. Boost-Type SMR

Power circuit configuration of a boost-type SMR is shown in Fig. 1. The circuit mainly consists of a diode bridge rectifier and a boost-type DC/DC converter. To simply the following theoretical analysis, some assumptions are made:

(i) the constituted circuit components in Fig. 1 are lossless;
(ii) the circuit includes a reasonably bulk capacitor C_d ;
(iii) the switch *SW* operates at infinity switching frequency;
(iv) without losing generality, the input voltage and input current of SMR are $v_s(t) = \hat{V}_s \sin(2\pi f_{in} t)$ and $i_s(t) = \hat{I}_s \sin(2\pi f_{in} t)$, respectively, where f_{in} is the input line frequency.

Then, the instantaneous input power and output power are equal and can be expressed as:

$$P(t) = 0.5\hat{V}_s\hat{I}_s - 0.5\hat{V}_s\hat{I}_s \cos(4\pi f_{in} t) \tag{1}$$

Thus, the average power $\overline{P} = 0.5\hat{V}_s\hat{I}_s$ is proportional to the input current magnitude $\hat{I}_s$ under constant input voltage magnitude $\hat{V}_s$.

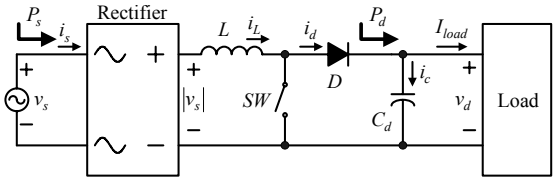

Fig. 1. Power circuit of the boost-type SMR.

As shown in Fig.2, the multi-loop control composes of inner current controller $G_{ci}(s)$ and outer voltage controller $G_{cv}(s)$. In order to regulate the output voltage v_d to desired command V_d^* , we can tune the input current command magnitude $\hat{I}^*$ through the voltage controller $G_{cv}(s)$. Multiplying $\hat{I}^*$ by the rectified sine signal $s(t)$ yields the desired inductor current command i_L^* for inner current controller $G_{ci}(s)$. Then, the switching signal $d(t)$ for switch *SW* in Fig.1 is generated by comparing the control signal v_{cont} and the triangular signal v_{tri} at the comparator's (+) terminal and (-) terminal, respectively.

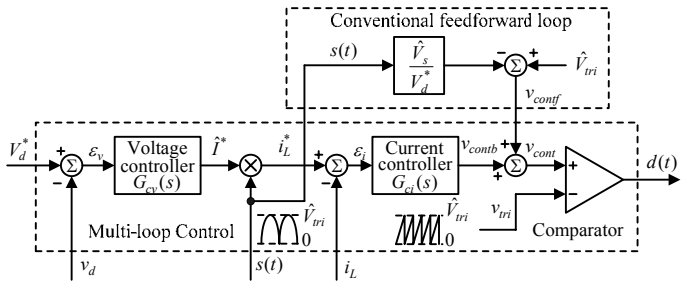

Fig. 2. Multi-loop control with conventional feedforward loop.

For the assumed infinity switching frequency, the instantaneous value of $|v_s(t)|$ can be seen as constant over one switching period and the average duty ratio $\bar{d}$ over one switching period can be expressed as

$$\bar{d} = \frac{v_{cont}}{\hat{V}_{tri}} \tag{2}$$

Because of the assumed bulk capacitor C_d and the use of voltage regulator, the output voltage v_d in steady state can be assumed to be equal to the desired dc voltage $v_d = V_d^*$. Accordingly, one can derive the following voltage equation using the averaging method:

$$L\frac{di_L}{dt} = |v_s| - (1-\bar{d})V_d^* \tag{3}$$

where L denotes the boosting inductance.

B. Multi-Loop Control without Feedforward Loop

By neglecting the feedforward loop in Fig. 2, the average duty ratio $\bar{d}(t)$ for multi-loop control without any feedforward loop can be expressed as:

$$\bar{d} = \frac{v_{contb}}{\hat{V}_{tri}} \tag{4}$$

where v_{contb} is the output of the feedback controller $G_{ci}(s)$ and $\hat{V}_{tri}$ denotes the magnitude of triangle signal v_{tri} and rectified sine signal $s(t) = \hat{V}_{tri}|\sin(2\pi f_{in} t)|$. Substituting (4) into (3) yields the following equation and gives the equivalent current control model plotted in Fig. 3.

$$L\frac{di_L}{dt} = \frac{v_{contb}}{\hat{V}_{tri}}V_d^* + (|v_s| - V_d^*) \tag{5}$$

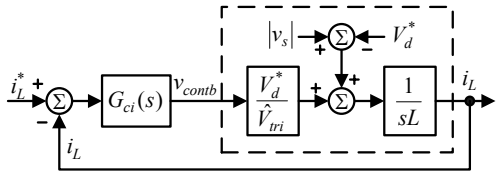

Fig. 3. Equivalent current control model without any feedforward loop.

The right term $(|v_s| - V_d^*)$ of (5) can be seen as a disturbance to the inner current controller. Fortunately, this disturbance and the current command i_L^* have the same function of $|\sin(2\pi f_{in} t)|$. It means that such disturbance is able to be removed by including a current command feedforward loop to the current control discussed in the following section.

C. Multi-Loop Control with Conventional Feedforward Loop

By considering the conventional feedforward loop shown in Fig. 2, the control signal v_{cont} now is the sum of the feedback control signal v_{contb} and the feedforward signal v_{contf} . Thus

the average duty ratio $\bar{d}$ with conventional feedforward loop now can be expressed by:

$$\bar{d} = \frac{v_{contf} + v_{contb}}{\hat{V}_{tri}} \tag{6}$$

In order to reject the disturbance in Fig. 3, the conventional feedforward signal v_{contf} (i.e. the nominal duty ratio pattern) is formulated as

$$v_{contf} = \hat{V}_{tri} - \hat{V}_{tri}\frac{\hat{V}_s}{V_d^*}\left|\sin(2\pi f_{in}t)\right| \tag{7}$$

From (7), we can find that the control feedforward signal v_{contf} is repeated with double line frequency $2f_{in}$. Since the variables in current loop such as i_L^*, i_L and v_{contb} are also repeated with the same frequency $2f_{in}$, we can substitute (6) and (7) into (3) to yield the following simplified equation,

$$L\frac{di_L}{dt} = \frac{V_d^*}{\hat{V}_{tri}}v_{contb} \tag{8}$$

Based on (8), the equivalent control model can be plotted in Fig. 4 where the disturbance shown in Fig. 3 is disappeared after introducing the conventional feedforward signal v_{contf}.

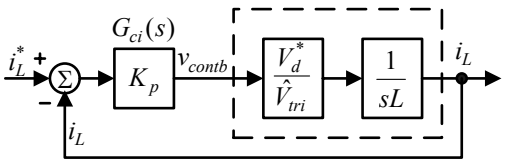

Fig. 4. Equivalent control model with conventional feedforward loop.

D. P-Type Current Feedback Controller

After applying the command feedforward loop in previous section, the tracking error due to disturbance in Fig. 3 can be greatly reduced and thus the simple P-type feedback controller $G_{ci} = K_p$ can be used to yield satisfactory control performance. Then, the closed-loop transfer function $T_p(s)$ for inductor current can be derived from Fig. 4 to be

$$T_p(s) = \frac{i_L(s)}{i_L^*(s)} = \frac{K_p V_d^*}{L\hat{V}_{tri}s + K_p V_d^*} = \frac{1}{1 + \frac{s}{(\frac{K_p V_d^*}{L\hat{V}_{tri}})}} \tag{9}$$

From (9), we can find that the transfer function $T_p(s)$ behaves like a low-pass filter and its cut-off frequency f_c in *Hz* is

$$f_c = \frac{K_p V_d^*}{2\pi L\hat{V}_{tri}} \tag{10}$$

It is noted that the cut-off frequency f_c is controllable by setting the parameter K_p. Furthermore, the input admittance $Y(s)$ of boost-type SMR with multi-loop control plus conventional feedforward loop can be expressed as

$$Y_f(s) = \frac{i_s(s)}{v_s(s)} = \frac{i_L(s)}{i_L^*(s)\frac{\hat{V}_s}{\hat{I}^*}} = \frac{\hat{I}^*}{\hat{V}_s}\frac{1}{1+\frac{s}{2\pi f_c}} \tag{11}$$

From (11), we can find that the SMR behaves like the pure resistor when input line frequency f_{in} is further smaller than the cut-off frequency f_c. It implies that the desired PFC function can be simply obtained by increasing f_c (i.e. by increasing P-type parameter K_p).

However, too large gain in practical control system would contribute to instability. In the design of feedback control gain, two key issues are additionally considered: (i) the current command i_L^* is a rectified sine signal with double line frequency $2f_{in}$; (ii) since the operation stability of a ramp-comparison PWM scheme is much affected by the P-type parameter K_p, a general criterion to determine the parameter is that the closed-loop cut-off frequency f_c must be less than the half of switching frequency $0.5f_{tri}$. In order to yield satisfactory current tracking switching control performance without sacrificing the switching operation stability, the frequency f_c with the conventional feedforward loop in (9) must be located at the range:

$$2f_{in} << f_c < 0.5f_{tri} \tag{12}$$

III. Proposed Phase Feedforward Control

Fig. 5 shows the proposed phase feedforward control (PFFC) for boost-type SMRs where its inner current controller is composed of a P-type feedback controller and a phase feedforward loop. From Fig. 5, the controllable phase θ is generated from the current magnitude command $\hat{I}^*$ and can be expressed as

$$\theta = \frac{2\pi f_{in}L}{\hat{V}_s}\hat{I}^* = \frac{\hat{I}^*}{\hat{I}_{short}} \tag{13}$$

where $\hat{I}_{short}$ is the peak current that will flow if the input voltage v_s was short circuited through boosting inductance L.

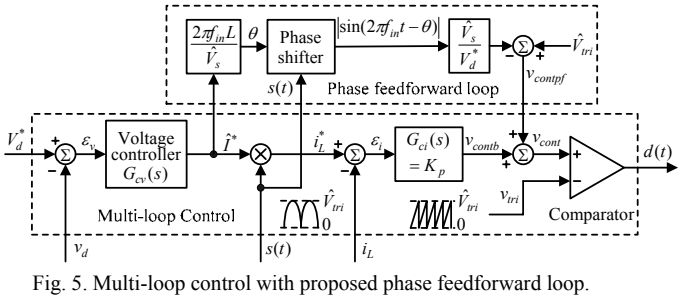

Fig. 5. Multi-loop control with proposed phase feedforward loop.

Then, the phase feedforward control signal v_{contpf} now becomes

$$v_{contpf} = \hat{V}_{tri} - \hat{V}_{tri}\frac{\hat{V}_s}{V_d^*}\left|\sin(2\pi f_{in}t - \theta)\right| \tag{14}$$

When the input line voltage is near zero, there is little voltage across the boost inductor L to drive current tracking the current command, even when switch SW is closed all the time. Therefore, the actual current may not be able to follow the desired current command which results in the cusp distortion. In [9], we find that the interval length φ in which cusp distortion occurs can be determined as follows:

$$\varphi = 2\tan^{-1}\left(\frac{\hat{I}^*}{\hat{I}_{short}}\right) = 2\tan^{-1}(\theta) \tag{15}$$

In order to attenuate the effect of cusp distortion on the current shaping performance, the interval length φ of cusp distortion in (15) should be kept near zero as possible as we can. Thus, it also implies that phase θ should also be near zero, too. Therefore, it is reasonable to assume that the phase θ in radians is near zero ($\theta \approx 0$) and therefore, $\sin\theta \approx \theta$ and $\cos\theta \approx 1$. By applying the above assumption into (14), the phase feedforward signal v_{contpf} can be approximated as

$$v_{contpf} \approx \hat{V}_{tri} - \hat{V}_{tri}\frac{\hat{V}_s}{V_d^*}\left|\sin(2\pi f_{in}t) - \theta\cos(2\pi f_{in}t)\right| \tag{16}$$

From the comparison between the conventional feedforward signal in (7) and the phase feedforward signal in (16), we can find that the two signals are similar except the term $\cos(2\pi f_{in}t)$ due to the introduced phase feedforward loop. By representing v_{contpf} in terms of v_{contf}, we can obtain

$$v_{contpf} = v_{contf} + \Delta v_f \tag{17}$$

where Δv_f denotes the difference between the proposed phase feedforward signal v_{contpf} and the conventional feedforward signal v_{contf}. Then, from (13), Δv_f can be expressed as

$$\Delta v_f \approx \text{sgn}[\sin(2\pi f_{in}t)]\frac{2\pi f_{in}L\hat{I}^*\hat{V}_{tri}}{V_d^*}\cos(2\pi f_{in}t) \tag{18}$$

where sgn[•] is the sign operator. The average duty ratio $\overline{d}$ in Fig. 5 now can be expressed by

$$\overline{d} = \frac{(v_{contb} + v_{contf} + \Delta v_f)}{\hat{V}_{tri}} \tag{19}$$

From (7) and (17)-(18), we can find that the feedforward signal Δv_f is repeated with the same double line frequency $2f_{in}$ as those variables in current loop such as i_L^*, i_L and v_{contb}. Thus, we can substitute (19) into (3) to yield the following equation:

$$L\frac{di_L}{dt} = \frac{V_d^*}{\hat{V}_{tri}}(v_{contb} + \Delta v_f) \tag{20}$$

Based on (20), the resulting equivalent current control dynamic model is shown in Fig. 6 where the inductor current command amplitude $\hat{I}^*$ is also plotted. Then, the closed-loop current tracking transfer function can be derived from Fig. 6 to be:

$$\frac{i_L(s)}{i_L^*(s)} = 1 \tag{21}$$

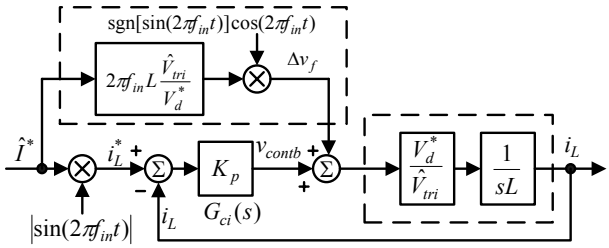

Fig. 6. Equivalent control model with proposed phase feedforward loop.

Equation (21) indicates that the proposed phase feedforward signal v_{contpf} in (16) can not only reject the disturbance in Fig. 3, but also completely achieve the dynamic response of the inductor current response. It also makes the input admittance of boost-type SMR with proposed PFFC to become

$$Y_{pf}(s) = \frac{i_s(s)}{v_s(s)} = \frac{\hat{I}^*}{\hat{V}_s} = \frac{\theta}{2\pi f_{in}L} \tag{22}$$

From (22), the input admittance $Y_{pf}(s)$ is real and constant over the entire frequency range of interests which implies that the proposed PFFC makes the boost-type SMR behave like a pure resistor.

However, we can also find that neither (21) nor (22) are dependent on the controller parameter K_p which do not imply that the current controller $G_{ci}(s)$ can be removed in practice due to the nonsinusoidal input voltage and nonideal circuit elements. Therefore, the role of current feedback controller $G_{ci}(s)$ in proposed PFFC is now changed from achieving the overall current response in (9) to compensating the effects of the practical circuit components.

Thus, since the most effort of feedback controller is alleviated through the proposed phase feedforward loop, the small parameter K_p can be used which is the another benefit of the proposed PFFC.

IV. Computer Simulation Study

In this section, we begin with a series of computer simulations to demonstrate the proposed PFFC. The circuit component values used are listed in Table I. It should be noted that no design optimization has been done in order to select the values in Table I. The PI-type controller is used as the voltage controller to regulate the output voltage.

By substituting the parameters in Table I into (10) and setting the closed-loop cut-frequency $f_c = 5\,kHz$ and $f_c = 0.5\,kHz$, respectively, the parameter of current controller $G_{ci}(s)$ can be obtained to be $K_p = 0.597$ and $K_p = 0.0597$, respectively. For cut-off frequency $f_c = 5\,kHz$ (i.e. $K_p = 0.597$), the simulated current waveforms without any feedforward loop, with conventional feedforward loop and with the proposed phase feedforward loop are plotted in Fig. 7(a)-(c), respectively.

Table I. Simulated circuit parameters

Input line voltage (peak)	$\hat{V}_s = 155V\ (110V_{rms})$
Triangular signal magnitude	$\hat{V}_{tri} = 1V$
Voltage command	$V_d^* = 250V$
Input line frequency	$f = 50Hz$
Smoothing capacitance	$C_d = 560\mu F$
Smoothing inductance	$L = 4.65mH$
Equivalent load resistance	$R_{load} = 100\Omega$
Carrier frequency	$f_{tri} = 25kHz$

In first, we can obviously find the current waveforms are improved through including both feedforward loops by comparing Fig. 7(a) with Fig. 7(b)-(c). However, negligible difference between the input current waveforms in Fig. 7(b) and in 7(c) can be found. Thus, for $f_c = 5\,kHz$, the response with conventional feedforward loop is much close to the response with the proposed phase feedforward loop which also demonstrates that (9) will approximately become (11) when the closed-loop cut-frequency is far larger than the line frequency $f_c (= 5kHz) >> f_{in} (= 50Hz)$.

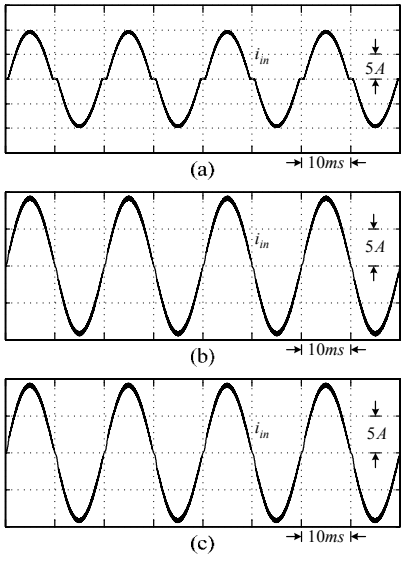

Fig. 7. Input currents for $f_c = 5\,kHz$:(a) without any feedforward loop; (b) with conventional feedforward loop; (c) with proposed phase feedforward loop.

In addition, the simulated waveforms for closed-loop cut-frequency $f_c = 0.5\,kHz$ are shown in Fig. 8. With comparison between Fig. 8(b) and Fig. 8(c), obvious current drops at zero-crossing points can be found in Fig. 8(b). Such current drops can not only contribute to the high harmonic currents but also result in additional power loss due to hard-switching of diode. It means that P-type current controller $G_{ci}(s)$ with conventional feedforward loop may not yield pure sine current waveforms when the closed-loop cut-frequency f_c is close to the line frequency f_{in} (i.e. when K_p is small). Furthermore, from Fig. 7(c) and Fig. 8(c), the current responses can be seen as identical to each other for various K_p which also demonstrates the pure response in (21). Thus, in order to obtain the desired current responses, small P-type parameter K_p can be used in the proposed PFFC which will increase the overall system stability.

Besides, the input harmonic currents of Fig. 8(b) and Fig. 8(c) are plotted in Fig. 9. From Fig. 9, we can find that the current waveform in Fig. 8(b) with conventional feedforward loop possesses higher harmonic currents than that in Fig. 8(c) with proposed phase feedforward loop under the same P-type parameter $K_p = 0.0597$.

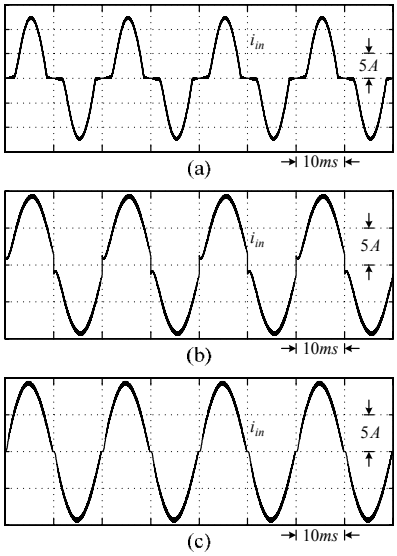

Fig. 8. Input currents for $f_c = 0.5\,kHz$:(a) without any feedforward loop; (b) with conventional feedforward loop; (c) with proposed phase feedforward loop.

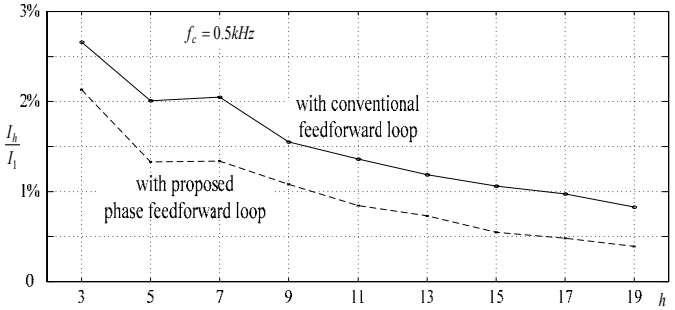

Fig. 9. Input harmonic currents with conventional feedforward loop and with proposed phase feedforward loop.

V. Experimental Results

The proposed PFFC has been digitally implemented in a DSP-based system using TMS320F240 where PI-type voltage

controller $G_{cv}(s)$ is used. In performing the digital control, the sampling frequencies set for the current loop and voltage loop are $25kHz$ and $1kHz$, respectively. In the hardware implementation, the component values are the same as listed in Table I where the output power is near $625W$. Some measured results are provided for demonstrating the control performances of the designed PFFC.

By setting closed-loop cut-frequency $f_c = 5\,kHz$ and $K_p = 0.597$, the measured input currents i_{in} with conventional feedforward loop and with proposed phase feedforward loop are plotted in Fig. 10(a) and 10(b), respectively. From Fig. 10, both feedforward loops can be seen as yielding the desired response.

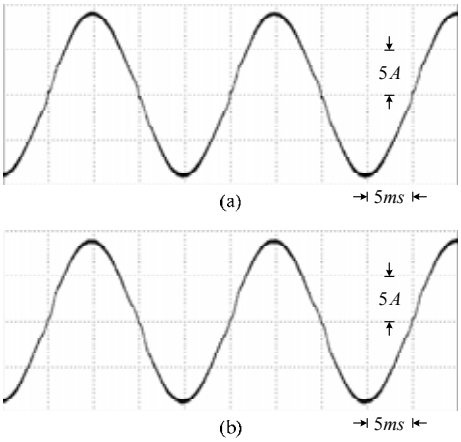

Fig. 10. Experimental input currents for $f_c \approx 5KHz$:(a) with conventional feedforward loop; (b) with proposed phase feedforward loop.

In addition, the input current responses with $f_c = 0.5\,kHz$ ($K_p = 0.0597$) for both feedforward loops are shown in Fig. 11(a) and 11(b), respectively. Even though the input current with the conventional feedforward loop is distorted in Fig. 11(a), the desired input current for the proposed PFFC still can be found in Fig. 11(b). It implies that the proposed phase feedforward loop can work well and yield the desired input current response for small K_p which shows the benefits of the proposed PFFC. Otherwise, when the cut-frequency f_c is far larger than the input line frequency f_{in} , both feedforward loops can obtain desired currents. But when the cut-frequency f_c is close to the input line frequency f_{in} , only proposed feedforward loop can be used.

VI. Conclusions

In this paper, the phase feedforward loop is proposed for digital implementation of PFC function. Based on the boost-type SMRs, the phase feedforward loop is derived in detail. By using the proposed phase feedforward loop, we can use economical P-type current controller with relatively small gain. Numerical simulation and experimental results further demonstrated and confirmed the benefits of the proposed PFFC, particularly for those applications whose current closed-loop cut-frequency is close to the input line frequency. Two specific applications where the proposed PFFC can be used are airborne systems and the low-cost digital control for 50-60Hz system. In the former, the input line frequency is high. For the latter, since the speed of DSP is no longer critical by using the proposed PFFC, the low-cost DSP can be used to implement PFC operation at high switching frequency.

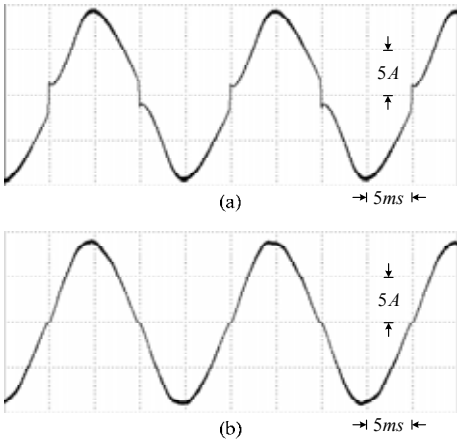

Fig. 11. Experimental input currents for $f_c \approx 0.5KHz$:(a) with conventional feedforward loop; (b) with proposed phase feedforward loop.

Acknowledgment

The author wish to thank the financial support under Grant NSC 96-2221-E-009-247 from the National Science Council in Taiwan.

References

[1] O. Garcia, J. A. Cobos, R. Prieto, P. Alou, and J. Uceda, 'Single phase Power Factor Correction: A Survey,' *IEEE Trans. on Power Electronics*, vol. 18, no. 3, pp. 749-754, May 2003.

[2] B. Singh, B. N. Singh, A. Chandra, K. Al-Haddad, A. Pandey, and D. P. Kothari, "A Review of Single-Phase Improved Power Quality AC-DC Converters", *IEEE Trans. on Industrial Electronics*, vol. 50, no. 5, pp. 962-981, October 2003.

[3] W. Zhang, G. Feng, Y. F. Liu, and B. Wu, "A digital Power Factor Correction (PFC) Control Strategy Optimized for DSP", *IEEE Trans. on Power Electronics*, vol. 19, no. 6, pp. 1474-1485, Nov. 2004.

[4] R. K. Tripathi, S. P. Das, and G. K. Dubey, "Mixed-Mode Operation of Boost Switch-Mode Rectifier for Wide Range of Load Variations", *IEEE Trans. on Power Electronics*, vol. 17, no. 6, pp. 999-1009, November 2002.

[5] H. C. Chen, S. H. Li, and C. M. Liaw, "Switch-Mode Rectifier with Digital Robust Ripple Compensation and Current Waveform Controls", *IEEE Trans. on Power Electronics*, vol. 19, no. 2, pp. 560-566, Mar. 2004.

[6] D. M. Van de Sype, K. De Gusseme, A. P. Van den Bossche, and J. A. Melkbeek, "Duty-Ratio Feedforward for Digitally Controlled Boost PFC Converters," *IEEE Trans. on Industrial Electronics*, vol. 52, no. 1, pp. 108-115, Feb. 2005.

[7] M. Chen, and J. Sun, "Feedforward Current Control of Boost Single-Phase PFC Converters", *IEEE Trans. on Power Electronics*, vol. 21, no. 2, pp. 338-345, Mar. 2006.

[8] E. Figueres, J. M. Benavent, G, Garcera, and M. Pascual "A Control Circuit With Load-Current Injection for Single-Phase Power-Factor-Correction Rectifiers", *IEEE Trans. on Industrial Electronics*, vol. 54, no. 3, pp. 1272-1281, June 2007.

[9] J. Sun, "Design and Analysis of Single-Phase PFC Converters for Airborne System," in *Proc. IEEE Industrial Electronics Conference,* 2003, pp. 1101-1109.